Experimental study on supersonic film cooling on the surface of a blunt body in hypersonic flow*

Fu Jia(付 佳), Yi Shi-He(易仕和)†, Wang Xiao-Hu(王小虎), He Lin(何 霖), and Ge Yong(葛 勇)

College of Aerospace Science and Engineering, National University of Defense Technology, Changsha 410073, *China*

(Received 19 November 2013; revised manuscript received 9 March 2014; published online 10 August 2014)

The experimental study focuses on the heat flux on a double cone blunt body in the presence of tangential-slot supersonic injection into hypersonic flow. The tests are conducted in a contoured axisymmetric nozzle with Mach numbers of 7.3 and 8.1, and the total temperature is about 900 K. The injection Mach number is 3.2, and total temperature is 300 K. A constant voltage circuit is developed to supply the temperature detectors instead of the normally used constant current circuit. The schlieren photographs are presented additionally to visualize the flow and help analyze the pressure relationship between the cooling flow and the main flow. The dependence of the film-cooling effectiveness on flow parameters, i.e. the blow ratio, the convective Mach number, and the attack angle, is determined. A semi-empirical formula is tested by the present data, and is improved for a better correlation.

Keywords: slot film cooling, hypersonic, schlieren visualization, cooling effectiveness

PACS: 47.15.gm, 44.10.+i, 47.55.pb, 47.27.te **DOI:** 10.1088/1674-1056/23/10/104702

1. Introduction

With the increasing interest in hypersonic atmospheric vehicles, aero-thermal protection becomes one of the most popular and important problems in this area. Film cooling is proved to be an effective technique which is widely used to protect engine components from the extreme thermal load,[1] and it is also used to prevent heat transfer to the sensor window on the surface of a hypersonic vehicle, such as the endoatmospheric homing interceptor.[2] If the temperature of the window reaches too high, the window will radiate into the sensor and act as a source of background noise, then the target signal-to-noise ratio (SNR) decreases. Also, the non-uniformly controlled temperature of the window can cause gradients in the window index of refraction, which can result in blurring or distortion.[3–5] Tangent slot film cooling is an effective method to solve both of these problems.

Since the middle of the last century, a lots of researches have been carried out on tangent slot film cooling. Wieghardt[6] performed the first study on this problem, and derived a similarity expression for the dimensionless gas phase temperature. Goldstein *et al.*[7] firstly defined film cooling as 'the employment of a secondary fluid injected through discrete slots to insulate thermally a solid surface from a gas stream flowing over it'. He also did comprehensive research on the film cooling effectiveness correlations.[7,8] Following these studies, more experimental researches have been done.[9–11] The possible factors that have an influence on the cooling effectiveness, such as the freestream and injection Mach numbers, total temperature, blow ratio, the height of slot, slot Reynolds number, etc., have been explored, and the way how they work has been studied in detail. For the convenience of engineering design, several semi-empirical cooling effectiveness correlations have been derived, but none of them could correlate all the data well for different experiment conditions and test facilities. In recent years, Maqbool *et al.*[12,13] and Fernando[14] designed experiments as the database to validate the computational results.

Meanwhile, to obtain a deep understanding of the flow field and benefit the quantitative analysis, different models of tangent slot film cooling were proposed,[14–17] which divide the flow field downstream of the slot into different areas based on different stages of the evolvement of velocity profile. With these models, the prediction of the flow field is supported with more physical background. The earlier numerical studies[18,19] are mainly based on the Reynolds Averaged Navier Stokes equations for kinds of flow conditions, and several turbulence models have been tested. In recent years, the large edgy simulation method has been developed rapidly, and begins to be applied to the prediction of the film cooling problem.[20,21] With these developments, the effects of pressure gradients, compressibility, density gradients, etc. on the film cooling effectiveness are explored quantitatively.[22]

In this paper we carry out an experimental study on the surface film cooling of a double cone blunt body, with a background of reducing the aero-optic effect that has mentioned above. A kind of constant voltage circuit is developed for the

*Project supported by the National Natural Science Foundation of China (Grant No. 11172326) and the Scientific Research Program of National University of Defense Technology, China (Grant No. 0100010112001).

†Corresponding author. E-mail: yishihe@gfkd.edu.cn, yishihe@nudt.edu.cn

© 2014 Chinese Physical Society and IOP Publishing Ltd

measurement of heat flux that is more economic than the commonly used constant current circuit. Various factors that influence the cooling effectiveness have been studied. The semi-empirical correlation reported by Majeski and Weatherford[2] for a similar model is tested for the present data. The correlation effect is discussed, and based on the discussion the formula is improved. The schlieren photographs are also taken to visualize the flow field.

2. General description

Although the tested model is axially symmetric, the structures of the film nozzle and tested surface have sufficient spans, which will be described in detail in the next part, so the film flow studied here can be regarded as being two-dimensional (2D). Furthermore, experiments are performed in low enthalpy condition to avoid any real gas effect, then the ideal gas behavior can be assumed. Based on this, a flow model and some main parameters will be introduced here.

The schematic diagram of the 2D film flow field is shown in Fig. 1. A cooling flow injected from the slot covers the surface to protect the window from being heated by the hot main flow. A shear layer will be formed between the two flows nearby the slot under the matched flow condition, which means that the static pressure of the film flow P_c and that of the main flow P_∞ are equal at the slot, and neither expansion nor compression of each flow will be performed. The wall temperature remains constant at the recovery value of the cooling flow in the potential core region. A laminar boundary layer of film flow exists in this region and merges with the free shear layer from the lip, which indicates the end of this region.[20] Large velocity and temperature gradients exist in the shear layer, but these are reduced at the wall by the low temperature of the cooling flow. With the distance from the slot increasing, the two flows mix and the gradients become smaller. When the flows mix fully in the boundary layer region, the profiles of the velocity and temperature are similar to those of the fully developed turbulence boundary layer, and the cooling effect will decrease fast. The over-expanded condition ($P_c/P_\infty<1$) of the film flow will promote the decrease, while the under-expanded condition ($P_c/P_\infty>1$) will delay the decrease.

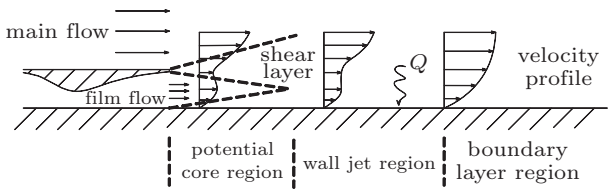


Fig. 1. Schematic diagram of 2D film flow structure.

The cooling effectiveness is influenced by many factors. One of the main parameters is the blowing ratio λ, which is defined as the specific mass flow ratio between the cooling gas and the free-stream:

$$\lambda = \frac{\rho_c u_c}{\rho_\infty u_\infty}. \tag{1}$$

Another parameter studied here is the attack angle. It is an important parameter because the aircraft should change attack angle frequently to follow the target while it is imaging-guided. Changing attack angle will change the flow field condition around the window, especially in the aero-thermal environment, which plays a key role in the imaging guidance. A large attack angle will raise the static pressure and temperature, and then the cooling effectiveness will decrease.

Other parameters considered but not studied specifically here include the main stream Mach number Ma, the convective Mach number M_c, and the slot height Reynolds number R_c. They will be discussed later.

The cooling effectiveness is defined in two different ways under different experimental conditions. For the present short duration facility, the experimental duration is in the order of millisecond, so the surface temperature change caused by the heat flux can be ignored, and the isothermal wall condition is assumed. The cooling effectiveness is then defined as

$$\eta = 1 - \frac{Q_c}{Q_0}, \tag{2}$$

where Q_c indicates the heat flux with cooling flow, and Q_0 the heat flux with main flow only.

3. Experimental procedure

3.1. Hypersonic gun tunnel

The experiments were conducted in the KD-01 hypersonic gun tunnel. It is a short-duration tunnel which consists of the gas source, the driving section, the driven section, the nozzle section, the experimental chamber, and the vacuum tank. The length of the whole tunnel is 42 m, and the inner diameters of driving and driven sections are both 103 mm. The diameter of nozzle exit is 500 mm, and the throat is changeable, so the Mach number is adjustable from 7 to 10. The tunnel runs with the free piston technique, which helps prolong the experiment time Δt to 30 ms with the present settings, meanwhile makes the flow conditions better.

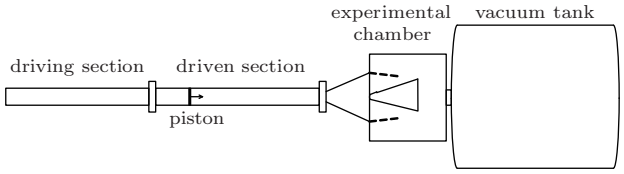


Fig. 2. Schematic diagram of KD-01 hypersonic gun tunnel.

In the present experiment, the Mach numbers are 7.3 and 8.1, and the total temperatures under the two Mach numbers

are both about 900 K. The detailed setup of the operating conditions is listed in Table 1. The values of these parameters are designed to be close to the really permitted flight conditions, as much as possible.

Table 1. Gun tunnel operating conditions.

Ma_∞	T_0/K	P_0/MPa	$Re_x/10^6$ m^{-1}	Δt/ms
7.3	899	7.0	15.2	25
8.1	907	8.9	13.8	30

3.2. Blunt body model and film cooling setup

The test model is a double cone blunt body, with a sphere head of 27.6 mm in radius, and the half cone angle of the fore-body is 15°, while that of the after-body is 7.53°. A flat space with a tangent rearward film slot slopes at 11.1° along the body. The structure of the film nozzle is 2D. The height of the slot h is 5 mm, the width is 32 mm, and the thickness of the slip is 0.5 mm. The exit direction of the nozzle is parallel to the window after the nozzle, of which the surface heat flux is to be measured. The Mach number at the exit of the nozzle is calibrated to be 3.2.

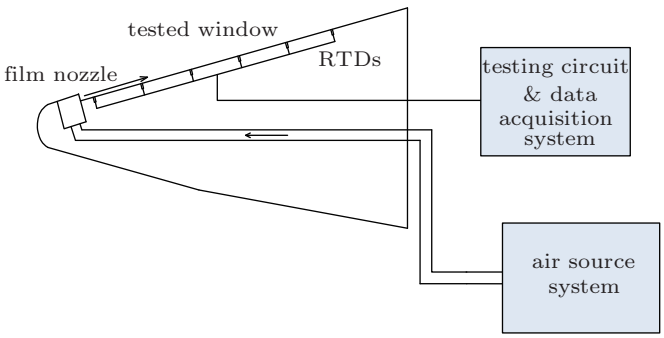


Fig. 3. Schematic illustration of the model.

The cooling system consists of the gas source, the pipeline, the film nozzle, and different kinds of valves. Several air bottles containing compressed air serve as the gas source, and they are connected to an iron pipe by oil pipes, through which the cooling gas will be transmitted to the film nozzle. The cooling gas is air and the total temperature is 300 K. The mass flow is controlled by a valve before the film nozzle. There is a pressure detector located in the plenum chamber to monitor the total pressure of the film flow.

3.3. Transient heat flux measurement technique

Platinum thin film resistance temperature detectors (RTDs) are used to measure the surface heat flux during the experiment. This kind of detector has an S-shape platinum film coated on a columnar Macor substrate with a length of 15 mm, and diameter of 2 mm, which enhances its sensitivity to temperature and ensures the one-dimensional (1D) heat conduction model valid. The resistance-to-temperature coefficients are different for different detectors, so it is calibrated in a constant temperature chamber for each detector before experiment. The calibration is carried out in a temperature range from 0 °C to 50 °C in steps of 10 °C, in which range the resistance changes during experiments.

Unlike the constant current circuit normally used in heat flux measurement, a constant voltage circuit is developed for the present test. The schematic plot is shown in Fig. 4. It basically consists of a constant voltage source and Wheatstone bridge units. The power is kept at a low voltage of 2 V to ensure that the self-Ohmic heating of the gauges is insignificant. The units are connected in parallel, so the real voltage applied to each bridge is less than 2 V and is measured before experiment. Each unit is composed of a thin film sensor R_d and three fixed resistances with an error of 0.1%. Two of the fixed resistances are both uniform 70 Ω, while the other resistance R_s is chosen to balance with the sensor, so that the output of the bridge will not go beyond the measuring range of the data acquisition system during experiment. The real time resistance of the sensor can be calculated by the following formula:

$$R_\mathrm{d}=\frac{(U_\mathrm{i}(R+R_\mathrm{s})+U_0R_\mathrm{s})R}{U_0R-U_\mathrm{i}(R_\mathrm{s}+R)}. \tag{3}$$

The temperature variation is calculated by the RTD resistance-temperature relationship:

$$\Delta T=\frac{\Delta R}{\alpha R_0}. \tag{4}$$

Then the heat flux can be derived by the heat transfer formulation of the detector:

$$q_\mathrm{w}=\sqrt{\frac{\rho ck}{\pi}}\left[\frac{\Delta T_\mathrm{w}(t)}{\sqrt{t}}+\frac{1}{2}\int_0^t\frac{\Delta T_\mathrm{w}(t)-\Delta T_\mathrm{w}(\tau)}{(t-\tau)^{3/2}}\mathrm{d}\tau\right]. \tag{5}$$

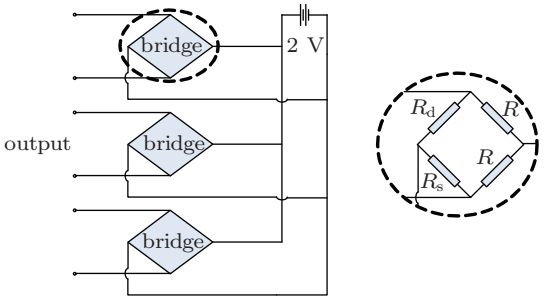


Fig. 4. Schematic plot of constant voltage heat flux measurement circuit.

Two DH5927 data acquisition systems with 32 channels in total are used to record the output voltage history of the bridge units. The sampling rate is 200 kHz. The voltage history data are downloaded to a PC immediately after the experiment. A numerical method developed by Cook and

Felderman[23] is used to solve the equation. The integral term in the equation is discretized in the following form:

$$\int_0^t \frac{\Delta T_{\rm w}(t)-\Delta T_{\rm w}(\tau)}{(t-\tau)^{3/2}}\,{\rm d}\tau = \sum_{i=1}^{n-1}\left(\Delta T_{\rm w}(t_{i+1})-\Delta T_{\rm w}(t_i)\right) \times\left[2(t_n-t_{i+1})^{-1/2}-2(t_n-t_i)^{-1/2}\right]. \quad (6)$$

The distribution of the RTDs is uniform along the central line of the tested surface, with an interval of 25.5 mm. The first gauge is located 8 mm away from the slot. Meanwhile, schlieren visualizations are used to monitor the flow, and the photographs are used to judge the relation between main flow static pressure and film flow static pressure qualitatively.

3.4. Measurement of flat plate heat transfer

The heat flux measurement system is tested by measuring the surface heat transfer of a flat plate with a leading edge angle of 15° for $Ma = 7.3$. The experimentally derived Stanton number is compared with theoretical estimation from the Eckert reference temperature method.[24] It is assumed that the formula of compressible flow heat transfer coefficient is similar to the incompressible one, and the parameter in the formula, which correlates with temperature and can be calculated by a characteristic temperature of the boundary layer instead, which is defined as the reference temperature T^*:

$$\frac{T^*}{T_{\rm e}} = 0.5 + 0.039M_{\rm e}^2 + 0.5\frac{T_{\rm w}}{T_{\rm e}}. \quad (7)$$

Using the Reynolds analogy, the theoretical Stanton number can be written as

$$St = \frac{1}{2}C_{\rm f}^* Pr^{*-2/3}, \quad (8)$$

where $C_{\rm f}^*$ indicates the reference local skin friction coefficient for laminar boundary-layer flow over a flat plate, and Pr^* the reference Prandtl number. Both of these two parameters are evaluated at reference temperature T^*. The $C_{\rm f}^*$ can be written as

$$C_{\rm f}^* = \frac{0.664}{\sqrt{Re_x^*}}\sqrt{C^*}, \quad (9)$$

where C^* indicates the Chapman–Rubesin factor[25] and is defined as

$$C^* = \frac{\rho^* u^*}{\rho_{\rm e} u_{\rm e}} \approx \left(\frac{T^*}{T_{\rm e}}\right)^{-1/3}. \quad (10)$$

The experimentally calculated Stanton number can be written as

$$St = \frac{q_{\rm w}}{\rho_\infty u_\infty c_{\rm p}(T_0 - T_{\rm w})}. \quad (11)$$

The experimental and theoretical results are shown in Fig. 5, and compared with those of Reddeppa and Gai.[25] They measured the surface heat flux of a backward facing step model with a leading edge angle of 25° for $Ma = 7.6$. Their results of upstream flat plate are comparable to the present ones. Since the structures of models and gauges are different, the tested sizes of their experiments are 5 mm∼48 mm, while the present ones are 95 mm∼275 mm. It has been found that the measured values match well with the theoretical estimation, and the experimental results are a little smaller than the theoretical values, which is the same with Reddeppa and Gai's.

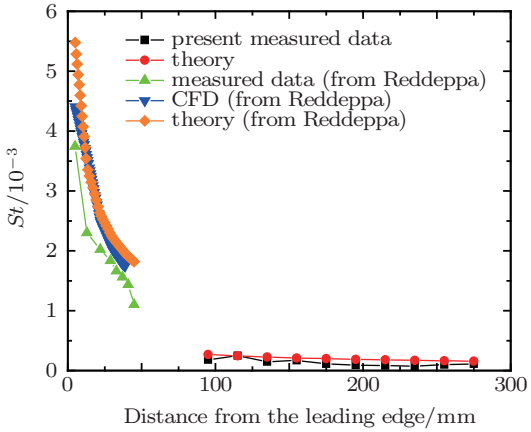


Fig. 5. (color online) Comparison of flat plate heat flux between our experimental and theoretical values and Reddeppa and Gai's.

4. Result analysis

4.1. Flow visualization

Schlieren visualizations are used to monitor the flow field and study the influence of different variables on the flow structure. For different attack angles and main streams, the experiments are conducted under three kinds of pressure conditions, i.e., the under-expanded condition, the over-expanded condition, and the matched condition. The judgment of different conditions is made qualitatively according to the angle of shear layer in the vicinity of the lip. The schlieren photographs of different pressure conditions with $\alpha = 0°$ under $Ma = 7.3$ are given in Fig. 6.

Figure 6(a) shows no film condition. The shock wave in the upper part of the flow field is the front shock induced by the blunt head of the model. A series of expansion waves is captured as the fan-shaped dark zone originating from the lip of the slot. The main flow reaches the tested surface and forms a reattachment shock wave. Figure 6(b) shows the over-expanded film condition. The shear layer shows a downward attitude angle relative to the surface before the slot. An expansion fan is still viewed under this condition. Figure 6(c) shows the matched film condition. The shear layer is nearly parallel to the upstream surface of the slot. The main flow is a little compressed at the slot by the film flow. Figure 6(d) shows the

scenario under the under-expanded film condition. The shear layer shows an upward angle relative to the upstream surface. A strong compressed shock wave is evident. By comparing Figs. 6(b) and 6(c), it can be found that the static pressure relation between the cooling film and the main flow has a significant influence on the structure of the flow field after the slot.

The attack angle also has an influence on the structure of the flow field. A larger angle will enhance the front shock and then the static pressure of the upstream before the slot increases, so with the same film mass flow, increasing the attack angle will reduce the static pressure ratio P_c/P_∞.

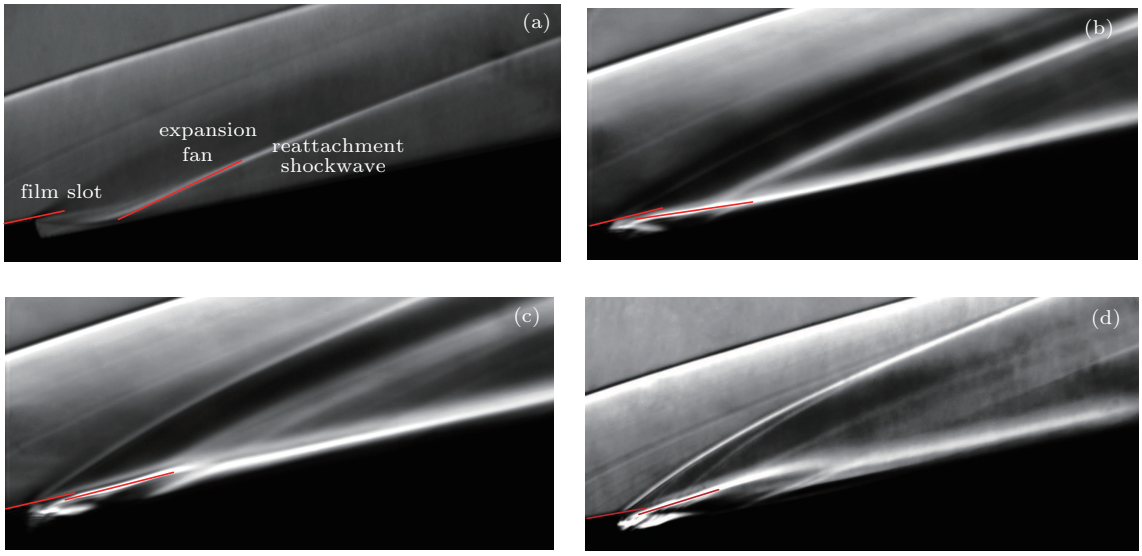


Fig. 6. (color online) Schlieren photographs of flow field under $Ma = 7.3$, $\alpha = 0^\circ$ for (a) $\lambda = 0$, (b) $\lambda = 1.14$, (c) $\lambda = 1.53$, (d) $\lambda = 3.94$.

4.2. Film cooling effectiveness correlation

Through the sixty-year studies of film cooling on various experiment facilities, main flow conditions, tested models and slot structures, and many empirical formulas of cooling effectiveness have been concluded under certain limitations. The purpose of establishing these formulas is to predict the film cooling effectiveness, but none of them can be used to predict all different conditions. For the problem of tangential film cooling on the surface of a blunt body, Majeski and Weatherford[2] concluded a sufficient formula, which was verified by a series of experimental and computational studies. The empirical formula is listed below:

$$\eta = aS^{*b}, \tag{12}$$

$$S^* = \left(\frac{x}{h\lambda}\right)\left(\frac{Re_c\mu_c}{\mu_e}\right)^{-0.25}\left(\frac{\rho_c}{\rho_e}\right)^{0.4} \times \left(\frac{\mu_e}{\mu_c}\right)^{0.75}\left(1+\frac{\gamma-1}{2}M_c^2\right)^{-0.5}. \tag{13}$$

Formula (12) shows that the relation between η and S^* follows a power form, which is widely accepted in current papers. S^* is a non-dimensional streamwise coordinate. The variable M_c is the convective Mach number, which is firstly proposed by Papamoschou,[26] Papamoschou and Roshko[27,28] and defined as

$$M_c = \frac{u_\infty - u_c}{a_\infty + a_c}. \tag{14}$$

This parameter correlates compressibility effect to cooling effectiveness. For the present experiment, the main flow Mach number, the film flow Mach number, and the total temperature are constant, then the constant convective Mach number can be deduced for the two mainstream conditions and different film conditions. The $M_{c,7} = 1.730$ when $Ma = 7.3$, while $M_{c,8} = 1.849$ when $Ma = 8.1$. Dellimore *et al.*[29] suggested that when $M_c > 1$, the compressibility effect is expected to be significant, and a strong compressibility will enhance the film cooling effectiveness by thinning the shear layer between the coolant and hot flow.

In formula (13), variable λ is the blow ratio, h is the slot height, μ_e and ρ_e are the viscosity coefficient and density of the main flow respectively, Re_c is the slot height Reynolds number, which is defined as

$$Re_c = \frac{\rho_c u_c h}{\mu_c}, \tag{15}$$

$\mu_c = 6.825 \times 10^{-6}$ kg·m^{-1}·s^{-1} is the viscosity coefficient of film flow. $\mu_{e,7} = 5.271 \times 10^{-6}$ kg·m^{-1}·s^{-1}, $\rho_{e,7} = 58$ g·cm^{-3} when $Ma = 7.3$, while $\mu_{e,8} = 4.304 \times 10^{-6}$ kg·m^{-1}·s^{-1}, $\rho_{e,8} =$

46 g·cm^{-3} when $Ma = 8.1$. The subscripts 7 and 8 of μ_e and ρ_e indicate the different conditions of these parameters for $Ma = 7.3$ and $Ma = 8.1$. The blow ratio λ, the slot height Reynolds number Re_c, and the film flow density ρ_c are related to film flow total pressure under different experiment conditions. The calculated blow ratios for different film total pressures are listed in Table 2. For the present gas source system, the blow ratio at more than 5 MPa is hard to achieve, so few data are obtained at larger value. Meanwhile, the over-expanded condition in which the window could not sufficiently cool down to reach the demand of application, so it is not tested for every condition. During experiment, we find that the matched condition can cool a large area, especially the small attack angle conditions, so it is tested for each main stream Mach number and attack angle, as well as the over-expanded condition.

Table 1. Summary of film flow conditions.

Main flow Ma	Attack angle/(°)	Blow ratio λ				
		Over-expanded	Matched		Under-expand	
7.3	0	1.14	1.53	2.15	2.52	3.94
	–2		1.59	2.38	2.56	3.90
	–4	–	2.06	2.50	3.62	3.88
	–10	2.36	4.66	5.10	–	–
8.1	0	1.30	1.59	1.90	3.14	
	–4	–	2.34	3.10	4.10	–
	–10	2.79/3.13	4.65	5.49	5.83	

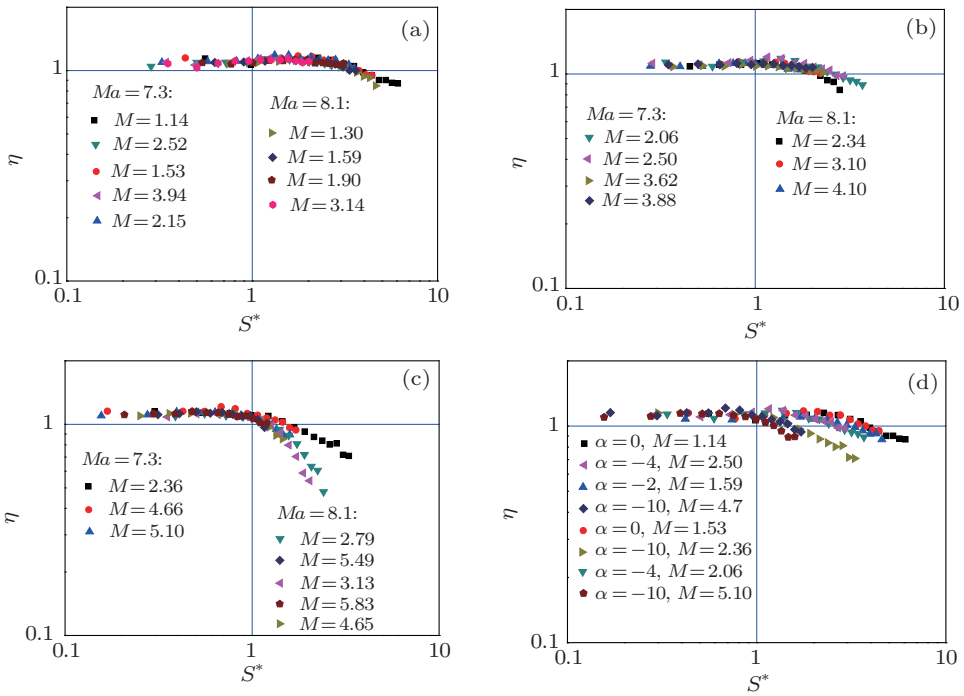


Fig. 7. (color online) η–S^* relation curves under attack angles of (a) $\alpha = 0°$, (b) $\alpha = -4°$, (c) $\alpha = -10°$, and under (d) Mach number of 7.3.

The non-dimensional coordinate S^* can be deduced from the data in the above table, and the cooling efficiency curves η–S^* in Fig. 7 are drawn in logarithmic coordinates. The variables a and b are uniformly set to be 1 here to emphasize the effect of correlation parameter S^*. Figures 7(a)–7(c) show the curves of different attack angles under different main stream Mach numbers and blow ratios. Under the attack angles of 0° and −4°, the curves correlate well, which can be seen from Figs. 7(a) and 7(b). Under the large attack angle of −10°, the curves are sensitive to the Mach number. The curves under different main flow conditions correlate well in the fully cooled area, but start to be divided into two tributaries at the point the curves accelerate the drop. Figure 8 shows the schlieren photographs of matched condition for attack angles of −4° and −10° under $Ma = 7.3$ and the adjusted angles of the photograph. Comparing Fig. 8(b) with Figs. 8(a) and 6(c), it is obvious that the shock layer for $\alpha = -10°$ is thinner and the shock wave interaction is more complex. The heat flux of the sur-

face far from the slot is dominantly influenced by the strongly shock-interacted flow, so the cooling effectiveness follows different curves for different main flow conditions. Figure 7(d) shows the curves under $Ma = 7.3$ with different attack angles and blow ratios. It can also be seen that the data do not correlate well for different attack angles, which implies that the formula is sensitive to attack angle.

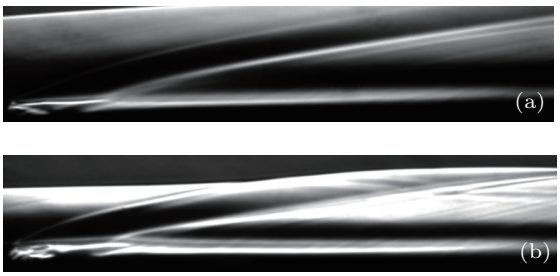


Fig. 8. Schlieren photographs of matched flow for $Ma = 7.3$ with attack angles of (a) $\alpha = -4°$ and $\lambda = 2.06$; (b) $\alpha = -10°$ and $\lambda = 4.66$.

The changes of variables a and b will change the position of the breakpoint and the curvature of the cooling curve, so an appropriate choice of these variables for different attack angles and main flow conditions may achieve a good correlation among different data. It is found that normalizing the values of correlation parameter S^* of different attack angles and setting the exponent b to be 1.3 for $Ma = 8.1$ while setting it to be 1 for $Ma = 7.3$ will correlate all the data well, as shown in Fig. 9.

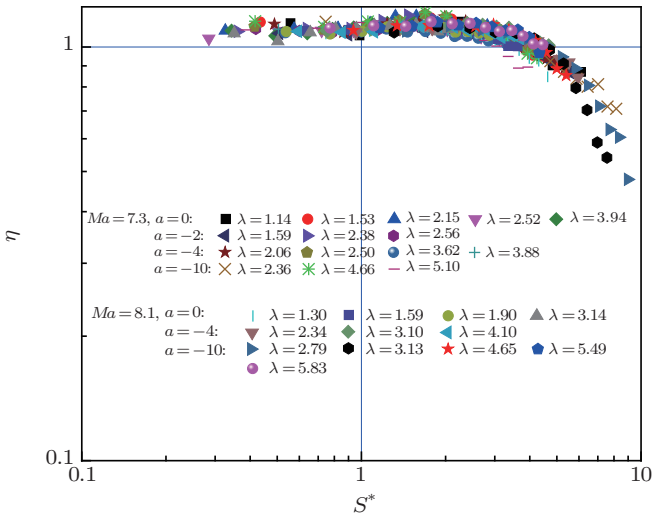


Fig. 9. (color online) η–S^* relation with normalized cooling length.

The normalization of S^* is to multiply it with the ratio of the cooling length S^*_{L} under a certain attack angle to that under the attack angle of 0° for $Ma = 7.3$. The ratio acts as the influence of the attack angle in which the original parameter S^* has not taken into consideration. For the present limited study, the cooling lengths for different attack angles and main flow conditions are shown in Fig. 10. The value for each attack angle is averaged by the tests at different blow ratios. Because for a certain attack angle, the values of parameter S^* can correlate well and the cooling lengths are the same. It can be seen that the cooling length curves under two different mainstream Mach numbers are similar.

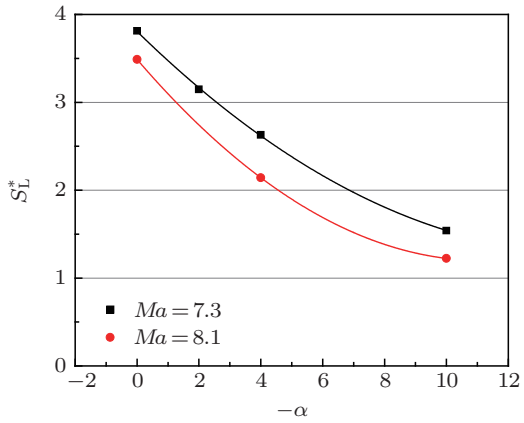


Fig. 10. (color online) Cooling lengths under different attack angles and main flow conditions.

4.3. Discussion

By analyzing formula (13), it can be found that the term (x/λ) mainly helps keep parameter S^* constant when the blow ratio changes. Then we can deduce that increasing the blow ratio will benefit the cooling effect, and lengthen the cooling length. This is because the large blow ratio means the large momentum of the film flow, and the surface will not be heated because most of the thermal energy from the main flow has been transported to the downstream before it reaches the tested window. However, excess blow ratio is not economic and will disturb the flow field, which can be seen from Fig. 6(d), and this will cause a complex aero-optical effect. To make comprehensive consideration, the matched condition may supply a sufficient cooling effect and a simpler flow field at the same time.

From the results in Subsection 4.2, it is known that formulas (12) and (13) fail to correlate the cooling effective curves of different attack angles and Mach numbers. It can be seen that the attack angle is not take into consideration in formula (13), but it is obvious that increasing the attack angle will increase the static pressure of the upstream around the slot, and the cooling effect must be affected. The cooling length is an important parameter which characterizes the point that divides the fully cooled area and the partially cooled area. From Fig. 10, it can be seen that the curves of S^*_{L}–α under different Mach numbers follow a similar regular pattern, so the cooling length is appropriate to be used to normalize the parameter S^*.

5. Conclusion

The effectiveness of film cooling is investigated experimentally in hypersonic gun tunnel KD-01. The influences of blow ratio and attack angle are studied in detail, and several conclusions can be reached from the present results.

Firstly, a constant voltage heat flux measurement circuit is developed to supply the sensors, and the data are calculated by numerical method. This circuit is identical to the constant current circuit technically, but it is lower-priced than the latter one and can be easily built in any relevant laboratory.

Secondly, the blow ratio plays a key role in cooling the window. Increasing the blow ratio can improve the effectiveness obviously, which means a lower thermal load and a longer cooling length. The attack angle has a great influence on the cooling effectiveness. Under a large attack angle, more mass flow of coolant gas is needed to reach the same level of cooling effectiveness under a small attack angle.

Thirdly, the semi-empirical correlation from Majeski and Weatherford[2] for a blunt cone model is tested with the present data. The correlation parameter S^* shows a sensitivity to attack angle and convective Mach number. Normalizing S^* with cooling length ratio and setting the power under $Ma = 8.1$ to be a certain value of 1.3 can correlate all the present data well. Furthermore, the curves of cooling length under different attack angles are found to be similar for the present two mainstream conditions.

References

[1] Carlos A C, Fernando R, Christopher C and Andre W M 2006 *IMECE*, November 5–10, 2006, Chicago, USA, 2006-15899

[2] Majeski J A and Weatherford R H 1988 *AIAA Thermophysics, Plasma Dynamics and Lasers Conference*, June 27–29, 1988, San Antonio, USA, 88-2624

[3] Zhu Y Z, Yi S H, Chen Z, Ge Y, Wang X H and Fu J 2013 *Acta Phys. Sin.* **62** 084219 (in Chinese)

[4] Zhu Y Z, Yi S H, He L, Tian L F and Zhou Y W 2013 *Chin. Phys. B* **22** 014702

[5] Gao Q, Yi S H, Jiang Z F, He L and Xie W K 2013 *Chin. Phys. B* **22** 014202

[6] Wieghardt K 1946 *AAF Trans. No.* F-TS-919-RE

[7] Goldstein R J, Eckert E R G, Tsou F K and Haji S A 1966 *AIAA Journal* **4** 981

[8] Goldstein R J 1971 *Film Cooling in Advances in Heat Transfer* (Vol. 7) (New York: Academic Press) pp. 321–378

[9] Richards B E and Stollery J L 1979 *Journal of Aircraft* **16** 177

[10] Bass R, Hardin L and Rodgers R 1990 *AIAA Second International Aerospace Planes Conferences*, October 29–31 Orlando, USA, 90-5239

[11] Juhany K A, Hunt M L and Sivo J M 1994 *J. Therm. Heat Transfer* **8** 59

[12] Maqbool D, Dellimore K and Cadou C 2010 46*th AIAA/ASME/SAE/ASEE Joint Propulsion Conference & Exhibit*, July 25–28, 2010, Nashville, USA, 2010-6886

[13] Maqbool D 2011 "Development of an Experiment for Measuring Film Cooling Performance in Supersonic Flows", M. S. Thesis (College Park: University of Maryland)

[14] Fernando R 2008 "Experimental Characterization of Slot Film Cooling Flows with Minimally Intrusive Diagnostic", M. S. Thesis (College Park: University of Maryland)

[15] Stollery J L, Ehwany E and A. A. M 1965 *Int. J. Heat Mass Transfer* **8** 55

[16] O'Connor J P and Haji-Sheikh A 1992 *AIAA Journal* **30** 2426

[17] Takeshi K, Goro M, Fumiei O and Yoshio W 1994 *J. Propulsion and Power* **10** 618

[18] Aupoix B, Mignosi A, Viala S, Bouvier F and Gaillard R 1998 *AIAA Journal* **36** 915

[19] Yang X B 2002 "Numerical Study of Film Cooling in Hypersonic Flows", Ph. D. Thesis (Glasgow: University of Glasgow)

[20] Konopka M, Meinke M and Schroder W 2010 46*th AIAA/ASME/SAE/ASEE Joint Propulsion Conference & Echibit*, July 25–28, 2010, Nashville, USA, 2010-6792

[21] Konopka M, Meinke M and Schroder W 2011 17*th AIAA Int. Space Planes and Hypersonic Sys. and Tech. Conf.*, April 11–14, 2011, San Francisco, USA, 2011-2250

[22] Dellimore K 2010 "Modeling and Simulation of Mixing Layer Flows For Rocket Engine Film Cooling", Ph. D. Thesis (College Park: University of Maryland)

[23] Cook W J and Felderman E J 1966 *AIAA Journal* **4** 561

[24] Eckert E 1955 *Journal of the Aeronautical Sciences* **22** 585

[25] Reddeppa P and Gai S L 2011 *J. Thermophys. Heat Transfer* **25** 321

[26] Papamoschou D 1986 "Experimental Investigation of Heterogeneous Compressible Shear Layers", Ph. D. Thesis (Pasadena: California Institute of Technology)

[27] Papamoschou D and Roshko A 1988 *Indian Academy of Sciences* **12** 1

[28] Papamoschou D and Roshko A 1988 *J. Fluid Mech.* **197** 453

[29] Kiran H, Dellimore K, André W, Marshall and Cadou C 2010 *J. Thermophys. Heat Transfer* **24** 3